Available online at www.sciencedirect.com
SCIENCE DIRECT®
Journal of Sound and Vibration 289 (2006) 229–244
JOURNAL OF SOUND AND VIBRATION
www.elsevier.com/locate/jsvi

Primary resonant optimal control for nested homoclinic and heteroclinic bifurcations in single-dof nonlinear oscillators

Hongjun Cao[a,*], Yaozhen Jiang[b], Yulin Shan[b]

[a]*Department of Mathematics, School of Science, Beijing Jiaotong University, Beijing 100044, PR China*
[b]*Department of Mathematics, Chuxiong Normal University, 461 Lucheng South Road, Chuxiong City 675000, Yunnan, PR China*

Received 19 October 2004; received in revised form 24 January 2005; accepted 17 February 2005
Available online 4 May 2005

Abstract

A unified control theorem is presented in this paper, whose aim is to suppress the transversal intersections of stable and unstable manifolds of homoclinic and heteroclinic orbits in the Poincarè map embedding in system dynamics. Based on the control theorem, a primary resonant optimal control technique (PROCT for short) is applied to a general single-dof nonlinear oscillator. The novelty of this technique is able to obtain the unified analytical expressions of the control gain and the control parameters for suppressing the homoclinic and heteroclinic bifurcations, where the control gain can guarantee that the control region where the homoclinic and heteroclinic bifurcations do not occur can be enlarged as much as possible at least cost. The technique is applied to a nonlinear oscillator with a pair of nested homoclinic and heteroclinic orbits. By the PROCT, the transversal intersections of homoclinic and heteroclinic orbits can be suppressed, respectively. The hopping phenomenon that there coexist two kinds of chaotic attractors of Duffing-type and pendulum-type can be suppressed. On the contrary, if the first amplitude coefficient is greater than the critical heteroclinic bifurcation value, then another degenerate hopping behavior of chaos will take place again. Therefore, the phenomenon of hopping is the dominant type of chaos in this oscillator, whose suppressing or inducing is admissible from the points of practical and theoretical view.

*Corresponding author. Tel.: +86 10 5168 2056; fax: +86 10 5168 8433.
E-mail address: hjcao@center.njtu.edu.cn (H. Cao).

0022-460X/$ - see front matter © 2005 Elsevier Ltd. All rights reserved.
doi:10.1016/j.jsv.2005.02.027

1. Introduction

There have been a lot of studies [1–7] show that the chaos resulted from homoclinic and heteroclinic bifurcations embedding in system dynamics can be suppressed by the addition of finite or infinite periodic excitations to a single-dof nonlinear oscillator. In particular, from Melnikov analysis [8,9], one can theoretically find the intervals of phase shift (initial phase difference) between the two excitations for which chaotic dynamics can be suppressed [3–5].

Recently, Lenci and Rega published a series of papers [10–12] concerning the optimal control for homoclinic or heteroclinic bifurcations in some classic and non-smooth nonlinear oscillators, respectively. The attention of this method proposed by Lenci and Rega is focused on choosing the optimal excitations with a finite number of superharmonics, by which the transversal intersection of the stable and unstable manifolds of the hilltop saddle in the Poincaré map can be avoided. Extensive numerical simulations have confirmed the effectiveness of the theoretical predictions of the method.

Based on the previous results, in this paper, a unified control theorem is presented for a general single-dof nonlinear oscillator. A primary resonant optimal control technique (PROCT for short) is proposed on the basis of Melnikov method and the phase shift between two primary resonant excitations. The aim of this technique is to control the transversal intersections of the stable and unstable manifolds of homoclinic and heteroclinic orbits embedding in system dynamics. The main scenario of this technique consists in the following steps: (i) by adding the second primary resonant excitation including a phase shift to the original system, via the Melnikov method and the rigorous mathematical deductions, the solutions of optimization problems can be luckily obtained, which means that the optimal amplitude coefficients as control parameters can be expressed as functions of the critical homoclinic/heteroclinic bifurcations as well as the phase shift in a optimal manner; (ii) once the phase shift as the original driven control parameter is chosen, a control gain that guarantees the region where the homoclinic or heteroclinic transversal intersections do not occur and two induced optimal control parameters are derived, and finally the control systems can be determined; (iii) by doing so, a control region is obtained, and associated with the parameter values in the region, the transversal intersections of the stable and unstable manifolds of the hilltop saddle in the Poincaré map of the system can be efficiently avoided.

Compared with Lenci and Rega's work, the main novelty of the PROCT is as follows: (i) by only adding the second primary resonant optimal excitation, and making use of the adjustable role played by the phase shift, the largest possible control gain can be attained at lowest cost; (ii) a unified analytical expression of optimization solutions of amplitudes can be obtained with respect to the suppression of homoclinic and heteroclinic bifurcations, simultaneously; (iii) using the PROCT, due to the amplitude coefficients depending on the phase shift and the critical homoclinic/heteroclinic bifurcation values under the harmonic excitation, they may always be adjusted in order that the amplitude coefficients are small enough, which is admissible from the physical and control points of view, and is also in accord with the assumption of the small perturbation in Melnikov theory.

The PROCT is applied to a nonlinear oscillator with a pair of nested homoclinic and heteroclinic orbits of unperturbed system. By the detailed theoretical analyses and numerical simulations, the transversal intersections of stable and unstable manifolds of homoclinic and heteroclinic can be successfully avoided, respectively. In addition, a novelty of this illustrative

example is that there exist two kinds of distinct interwinding chaotic attractors when the critical homoclinic bifurcation values are further increased to the critical heteroclinic bifurcation values, that is Duffing-type and pendulum-type, simultaneously. By using the PROCT, the hopping behavior of chaos occurred in this example can be suppressed, and in general can be transformed into the quasiperiodic motions.

The rest of this paper is organized as follows: Section 2 presents the unified control theorem and the theoretical analysis of the PROCT for a general one-dof nonlinear oscillator. Section 3 is devoted to an illustrative example, in which a pair of nested homoclinic and heteroclinic bifurcations can be effectively suppressed, respectively. Finally, some conclusions and comments are given in Section 4.

2. Theoretical analysis on the primary resonant optimal control technique

A general one-dof nonlinear oscillator is considered in the following form:

$$\begin{aligned} \dot{x} &= y, \\ \dot{y} &= -g(x) - \delta h(x)y + \gamma_1 \cos(\omega t) + \gamma_2 \cos(\omega t + \Psi), \end{aligned} \tag{1}$$

where $g(x)$ is a potential function, $\delta h(x)y$ represents a weak damping term, with a nonlinear damping function $h(x)$ and a parameter δ denoting the damping intensity, $\gamma_1 \cos(\omega t)$ is named the harmonic excitation, ω is a forced frequency, and $\gamma_2 \cos(\omega t + \Psi)$ is called the second primary resonant periodic excitation, and Ψ is a phase shift between the first harmonic excitation and the second primary resonant period excitation. In addition, δ, γ_1 and γ_2 are small enough parameter.

It can be easily seen that the Duffing oscillator, the van der Pol oscillator, the Duffing–Van del Pol oscillator, and the pendulum equation are all special cases of Eq. (1).

At first, the following hypotheses and properties are presented concerning the general one-dof nonlinear oscillator (1):

(i) Suppose that $g(-x) = -g(x)$ and $h(-x) = h(x)$;

(ii) The unperturbed and undamped system of Eq. (1) has one pair of homoclinic orbits $\Gamma^{r,l} = (x_0^{r,l}(t), y_0^{r,l}(t))$ (or one pair of heteroclinic orbits $\Gamma^{\text{up,low}} = (x_0^{\text{up,low}}(t), y_0^{\text{up,low}}(t))$) connecting a hyperbolic saddle point S_0^0 (or a pair of saddle points S_{-1}^0 and S_1^0), where the superscripts "r", and "l" denote the right, left homoclinic orbits of unperturbed system, and "up", and "low" denote the upper and the lower heteroclinic orbits of unperturbed system, respectively.

(iii) $x_0^{r,l}(-t) = x_0^{r,l}(t)$, $y_0^{r,l}(-t) = -y_0^{r,l}(t)$,

(iv) $x_0^{\text{up,low}}(-t) = x_0^{\text{up,low}}(t)$, $y_0^{\text{up,low}}(-t) = y_0^{\text{up,low}}(t)$.

(v) Eq. (1) is invariant under the transformation $x \to -x$, $t \to t + \pi/\omega$, which means that there exists a pair of symmetric homoclinic orbits or a pair of symmetric heteroclinic orbits of unperturbed system of Eq. (1).

Firstly, for the homoclinic case, Melnikov's theory [8,9] guarantees that, in the small enough perturbation, there exist homoclinic intersections of the stable and unstable manifolds in the Poincaré map of the system if and only if $M^{r,l}(t_0)$ have a simple zero for some t_0. Then, Melnikov

functions for Eq. (1) are as follows:

$$\begin{aligned} M^{r,l}(t_0) = & \int_{-\infty}^{\infty} y_0^{r,l}(t)\{-\delta h(x_0^{r,l}(t))y_0^{r,l}(t) \\ & \pm(\gamma_1 \cos\omega(t+t_0)+\gamma_2 \cos(\omega(t+t_0)+\Psi))\}\,\mathrm{d}t \\ = & -\delta\int_{-\infty}^{\infty} h(x_0^{r,l}(t))[y_0^{r,l}(t)]^2\,\mathrm{d}t \pm \left[\gamma_1 \sin(\omega t_0)\int_{-\infty}^{\infty} y_0^{r,l}(t)\sin(\omega t)\,\mathrm{d}t \right. \\ & \left. +\gamma_2 \sin(\omega t_0)\int_{-\infty}^{\infty} y_0^{r,l}(t)\sin(\omega t+\Psi)\,\mathrm{d}t\right]. \end{aligned} \tag{2}$$

For simplicity, some notations are introduced as follows

$$\begin{aligned} B^{r,l} &= \int_{-\infty}^{\infty} h[x_0^{r,l}(t)][y_0^{r,l}(t)]^2\,\mathrm{d}t, \\ I_1^{r,l}(\omega) &= \int_{-\infty}^{\infty} y_0^{r,l}(t)\sin(\omega t)\,\mathrm{d}t, \\ h_2^{r,l}(\omega) &= \frac{\gamma_{2,\mathrm{cr}}^{r,l}}{\gamma_{1,\mathrm{cr}}^{r,l}}, \\ \gamma_{1,\mathrm{crh}}^{r,l}(\omega) &= \frac{\delta B^{r,l}}{I_1^{r,l}(\omega)}, \end{aligned} \tag{3}$$

where $\gamma_{1,\mathrm{crh}}^{r,l}(\omega)$ represent the critical right/left homoclinic bifurcations in the action of simply a harmonic excitation. $\gamma_{1,\mathrm{cr}}^{r,l}$ and $\gamma_{2,\mathrm{cr}}^{r,l}$ denote the critical right/left homoclinic bifurcations under the action of the two primary resonant excitations. In addition, $h_2^{r,l}(\omega)$ measure the effect of the second primary resonant harmonic corrections on the Melnikov's functions $M^{r,l}(t_0)$, respectively.

Then Eq. (2) becomes

$$M^{r,l}(m) = -\delta B\left[1 \pm \frac{\gamma_1}{\gamma_{1,\mathrm{crh}}^{r,l}(\omega)}\,h^{r,l}(m)\right], \tag{4}$$

where

$$h^{r,l}(m) = \sin(m) + h_2^{r,l}\,\sin(m+\Psi), \tag{5}$$

and $m = \omega t_0$ ($m \in [0, 2\pi]$). $h(m)$ is 2π-periodic and has zero mean value, and the effects of the second primary resonant excitation in the Melnikov function are governed by the parameters $h_2^{r,l}$ and Ψ.

Similarly, for the heteroclinic case, in order to avoid the unnecessary repetition, the same notations given in Eq. (3) are still used, and the only difference is to change the superscript "r" and "l" into "up" and "low" denoting the upper and lower heteroclinic orbits. In addition, the superscripts "hom" and "hete" denote the homoclinic and heteroclinic orbit, respectively.

Melnikov functions with respect to the heteroclinic case for Eq. (1) are as follows:

$$M^{\mathrm{up,low}}(t_0) = -\delta B\left[1 \pm \frac{\gamma_1}{\gamma_{1,\mathrm{crh}}^{\mathrm{up,low}}(\omega)}\, h^{\mathrm{up,low}}(m)\right], \tag{6}$$

where

$$h^{\mathrm{up,low}}(m) = \cos(m) + h_2^{\mathrm{up,low}}\, \cos(m + \Psi). \tag{7}$$

The following definition is given:

Definition 1. Let

$$\begin{aligned}
&M^r := -\min_{m\in[0,2\pi]}\{h^r(m)\}, \quad M^l := \max_{m\in[0,2\pi]}\{h^l(m)\},\\
&M^{\mathrm{up}} := -\min_{m\in[0,2\pi]}\{h^{\mathrm{up}}(m)\}, \quad M^{\mathrm{low}} := \max_{m\in[0,2\pi]}\{h^{\mathrm{low}}(m)\},\\
&G^r := \frac{\gamma_{1,\mathrm{crh}}^r(\omega)}{\gamma_1^r(\omega)} = \frac{1}{M^r}, \quad G^l := \frac{\gamma_{1,\mathrm{crh}}^l(\omega)}{\gamma_1^l(\omega)} = \frac{1}{M^l},\\
&G^{\mathrm{up}} := \frac{\gamma_{1,\mathrm{crh}}^{\mathrm{up}}(\omega)}{\gamma_1^{\mathrm{up}}(\omega)} = \frac{1}{M^{\mathrm{up}}}, \quad G^{\mathrm{low}} := \frac{\gamma_{1,\mathrm{crh}}^{\mathrm{low}}(\omega)}{\gamma_1^{\mathrm{low}}(\omega)} = \frac{1}{M^{\mathrm{low}}},
\end{aligned} \tag{8}$$

where $G^{r,l}$ and $G^{\mathrm{up,low}}$ are named the control gain.

Due to the symmetric property (v), it is easy to prove the following conclusion:

Proposition 1.

$$\begin{aligned}
&M^r = M^l := M^{\mathrm{hom}}, \quad M^{\mathrm{up}} = M^{\mathrm{low}} := M^{\mathrm{hete}},\\
&G^r = G^l := G^{\mathrm{hom}}, \quad G^{\mathrm{up}} = G^{\mathrm{low}} := G^{\mathrm{hete}}.
\end{aligned}$$

The control gain G can measure the increment of critical threshold with respect to the reference harmonic excitation after the second excitation is added. Seen from Eq. (8), the smaller the M^{hom} and M^{hete}, the larger the control gain G^{hom} and G^{hete}. Therefore, once the M^{hom} and M^{hete} are determined, then the control gain G^{hom} and G^{hete} are determined too. Finally, the control (or *saved*) region above $\gamma_{1,\mathrm{crh}}^{\mathrm{hom,hete}}(\omega)$ and below $\gamma_{1,\mathrm{cr}}^{\mathrm{hom,hete}}(\omega)$ can be obtained. Therefore, corresponding to the control parameters in the control region, the transverse intersections of the stable and unstable manifolds of the hilltop saddle in the Poincaré map of the system can be successfully avoided in theory.

In the following discussion, the key of the PROCT is to solve the following optimization problem:

2.1. Maximizing G by varying h_2 and Ψ of $h(m)$ as given in Eqs. (5) and (7)

The solutions of optimization problem can be obtained by the following unified control theorem:

Theorem. *When* $h_2 = -\cos(\Psi)$, *the function* $h(m)$ *given in Eqs.* (5) *and* (7) *can attain its maximum* $|\sin(\Psi)|$, *and the following formulae holds*:

$$M^{\mathrm{hom}} = M^{\mathrm{hete}} =: M = |\sin(\Psi)|, \tag{9}$$

and the control gain is $G = 1/|\sin(\Psi)|$, *where* Ψ *is confined in the interval of* $(0, \pi/2)$.

Proof. Firstly, for the homoclinic case, from Eq. (5), it is easy to know that when

$$\sin^2(m) = \frac{(1 + h_2 \cos \Psi)^2}{(1 + h_2 \cos \Psi)^2 + (h_2 \sin \Psi)^2},$$
$$\cos^2(m) = \frac{(h_2 \sin \Psi)^2}{(1 + h_2 \cos \Psi)^2 + (h_2 \sin \Psi)^2}, \tag{10}$$

$\mathrm{d}h/\mathrm{d}m = 0$ has zero points. Substituting Eq. (10) into Eq. (5), the following inequality

$$h(m) = \sqrt{(h_2 + \cos \Psi)^2 + \sin^2 \Psi} \leqslant |\sin \Psi|, \tag{11}$$

holds if and only if $h_2 = -\cos \Psi$.

Similarly, for the heteroclinic case, $\mathrm{d}h/\mathrm{d}m = 0$ has zero points when two equations given in Eq. (10) are satisfied. Substituting Eq. (10) into Eq. (7), one has

$$h(m) = \frac{(1 + h_2 \cos \Psi)^2 - (h_2 \sin \Psi)^2}{\sqrt{(1 + h_2 \cos \Psi)^2 + (h_2 \sin \Psi)^2}}, \tag{12}$$

and the following inequality

$$|h(m)| \leqslant \frac{(1 + h_2 \cos \Psi)^2 + (h_2 \sin \Psi)^2}{\sqrt{(1 + h_2 \cos \Psi)^2 + (h_2 \sin \Psi)^2}} = \sqrt{(h_2 + \cos \Psi)^2 + \sin^2 \Psi} \leqslant |\sin \Psi|, \tag{13}$$

holds if and only if $h_2 = -\cos \Psi$. □

Once the control gain G and the coefficient h_2 are obtained, by using the third and the fourth equations given in Eq. (3), the optimal control amplitude coefficients are derived by

$$\gamma_{1,\mathrm{cr}}^{\mathrm{hom,hete}} = \gamma_{1,\mathrm{crh}}^{\mathrm{hom,hete}}(\omega) G = \frac{1}{|\sin(\Psi)|} \gamma_{1,\mathrm{crh}}^{\mathrm{hom,hete}}(\omega) > \gamma_{1,\mathrm{crh}}^{\mathrm{hom,hete}},$$
$$\gamma_{2,\mathrm{cr}}^{\mathrm{hom,hete}} = \gamma_{1,\mathrm{cr}}^{\mathrm{hom,hete}} h_2 = -\cos(\Psi) \gamma_{1,\mathrm{cr}}^{\mathrm{hom,hete}}. \tag{14}$$

As can be seen from the first equation of Eq. (14), due to the effect of the control gain G, the first optimal control amplitude coefficient $\gamma_{1,\mathrm{cr}}^{\mathrm{hom,hete}}$ will be increased. Subsequently, the zone of transversal intersection of homoclinic and heteroclinic manifolds will be decreased as much as possible. Substituting Eq. (14) into Eq. (1), the optimal control system for suppressing homoclinic and heteroclinic bifurcations is

$$\dot{x} = y,$$
$$\dot{y} = -g(x) - \delta h(x) y + \gamma_{1,\mathrm{cr}}^{\mathrm{hom,hete}} \cos(\omega t) + \gamma_{2,\mathrm{cr}}^{\mathrm{hom,hete}} \cos(\omega t + \Psi). \tag{15}$$

3. An illustrative example

To show the effectiveness of the primary resonant optimal control technique and the agreement between the theoretical analyses and the numerical simulations, in this section, consider an

illustrative nonlinear oscillator with a pair of nested homoclinic and heteroclinic orbits of unperturbed system, simultaneously, whose dimensionless equation is below

$$\begin{aligned}\dot{x} &= y,\\ \dot{y} &= \sin x(\cos x - \alpha^2) - \delta y + \gamma_1 \cos(\omega t) + \gamma_2 \cos(\omega t + \Psi),\end{aligned} \tag{16}$$

where a small parameter $0<\varepsilon\ll 1$ is introduced, and assume that $\delta = O(\varepsilon)$, and $\gamma_j = O(\varepsilon)$ $(j = 1, 2)$ but $\alpha, \omega = O(1)$. Here in order to guarantee that there exist a nested homoclinic and heteroclinic orbits simultaneously, α is assumed to be satisfied the condition $|\alpha|<1$. Physically, α is the radius of the wire, δ represents the damping coefficient, γ_j the amplitude of the forcing corresponding to different periodic excitations, ω the frequency.

Eq. (16) is in fact a specific case of the following dimensionless equation:

$$\begin{aligned}\dot{x} &= y,\\ \dot{y} &= \sin x(\cos x - \alpha^2) - \delta y + \beta\delta(1 - \cos 2x)y + \gamma_1 \cos(\omega t).\end{aligned} \tag{17}$$

An important result obtained by Dabbs and Smith [13] was: for Eq. (17), two distinct types of horseshoes, namely Duffing oscillators and pendulum type are shown to coexist. Some special parameter relationships predict that both types of horseshoes coexist but do not interact despite very large forcing amplitudes.

Here, for simplicity, the main interest of this paper is to suppress the homoclinic and heteroclinic bifurcation embedding in system dynamics respectively, so only a damping term δy is considered in Eq. (16).

System (16) is invariant under the transformation $x \to -x$, $t \to t + \pi/\omega$ which guarantees all homoclinic and heteroclinic orbits of unperturbed system are symmetric.

3.1. Undamping and unforced system of Eq. (16)

In the forthcoming part of this subsection, all parameter values are assumed as $\alpha = 0.5$, and $\delta = 0.1$. When $\delta = 0$ and $\gamma_j = 0$ $(j = 1, 2)$, the undamping and unforced system, that is, the unperturbed system of Eq. (16) is

$$\begin{aligned}\dot{x} &= y,\\ \dot{y} &= \sin x(\cos x - \alpha^2).\end{aligned} \tag{18}$$

The unperturbed system (18) corresponds to an integrable Hamiltonian system with the potential function

$$V(x) = -\tfrac{1}{2}(\sin x)^2 - \alpha^2 \cos x, \tag{19}$$

and the Hamiltonian function (energy)

$$H(x, y) = \frac{y^2}{2} - \frac{1}{2}(\sin x)^2 - \alpha^2 \cos x. \tag{20}$$

From Eqs. (18)–(20), the unperturbed system (18) has five equilibrium points when $x \in [-4, 4]$: two centers at $C^0_{-1}(-1.31812, 0)$ and $C^0_1(1.31812, 0)$, and three hyperbolic saddle points at $S^0_{-1}(-\pi, 0)$, $S^0_0(0, 0)$, and $S^0_1(\pi, 0)$. In addition, in order to compute Melnikov functions in the

subsequent parts, three turning points $T^0_{-1}(-2.0944, 0)$, $T^0_1(2.0944, 0)$, and $T^0_0(0, 1)$ are given. The saddle point S^0_0 is connected to itself by two symmetric homoclinic orbits $\Gamma^{r,l}_0 = (x^{r,l}_0(t), y^{r,l}_0(t))$, and the other saddle points S^0_{-1}, S^0_1 are connected by two symmetric heteroclinic orbits $\Gamma^{\text{up,low}}_0 = (x^{\text{up,low}}_0(t), y^{\text{up,low}}_0(t))$.

The oscillation frequency is $\omega^{r,l}_0 = 0.9682$ occurred in twin-well potential wells, respectively. In this paper, only the primary resonant condition $\omega \simeq \omega^{r,l}_0 + \sigma$ is considered, where σ is a small enough parameter.

For a clear illustration, it is useful to present computational results of the phase space of unperturbed system (18) shown in Fig. 1 within the region $-4 \leqslant x \leqslant 4$ and $-1.5 \leqslant y \leqslant 1.5$, which is only a restricted portion by cutting the cylindrical space. Seen from Fig. 1, there exist two kinds of oscillations, one is the oscillation within the twin-well potential wells, respectively; one is the oscillation between the homoclinic orbits $\Gamma^{r,l}_0$ and the heteroclinic orbits $\Gamma^{\text{up,low}}_0$. In addition, there still exists another rotation outside the heteroclinic orbits $\Gamma^{\text{up,low}}_0$.

3.2. Melnikov analysis for Eq. (16)

By Melnikov analysis given in Section 2, Fig. 2 shows the critical values for homoclinic and heteroclinic bifurcations $\gamma^{r,l}_{1,\text{crh}}$, $\gamma^{r,l}_{1,\text{cr}}$, and $\gamma^{\text{up,low}}_{1,\text{crh}}$, $\gamma^{\text{up,low}}_{1,\text{cr}}$ as functions of frequency ω under the action of a harmonic excitation, and a harmonic and a primary resonant excitation, respectively, in which the solid curve corresponds to the homoclinic bifurcation, and the dashed curve denotes the heteroclinic bifurcation. Comparison between them, as the frequency ω is in the interval $(0, 0.2408)$, the homoclinic bifurcation values are larger than the heteroclinic bifurcation value. While, there exist one critical homoclinic bifurcation $\gamma_{1,\text{crh}} = 0.1046$ at $\omega = 0.2408$ such that the

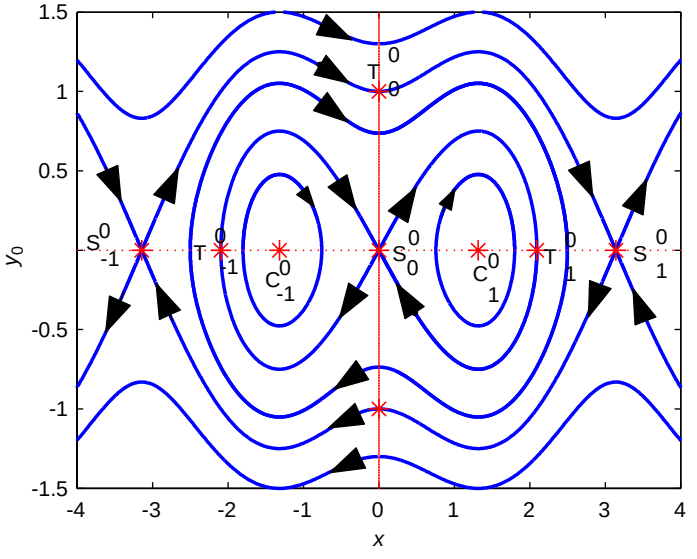

Fig. 1. The unperturbed phase space when $\alpha = 0.5$.

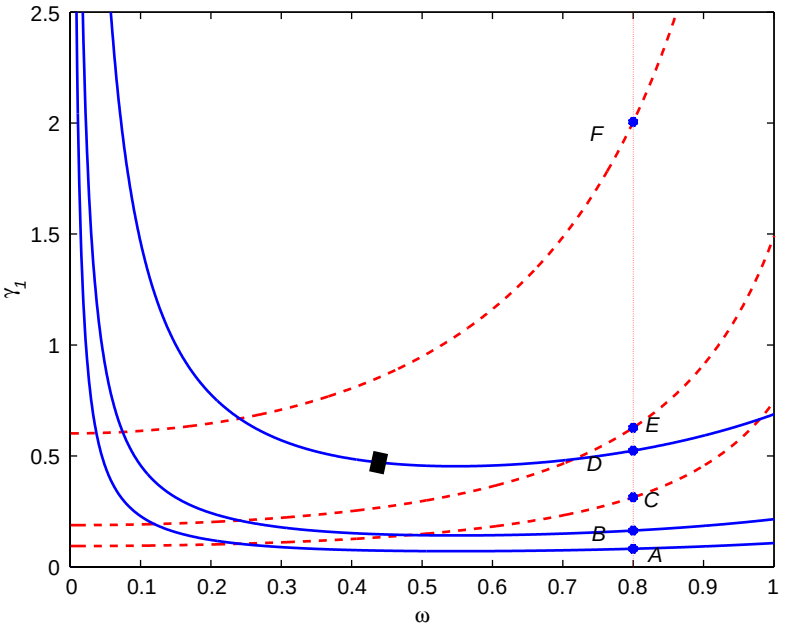

Fig. 2. Homoclinic bifurcation curves $\gamma_{1,\mathrm{crh}}^{\mathrm{hom}}$ and $\gamma_{1,\mathrm{cr}}^{\mathrm{hom}}$ are shown in solid curves; heteroclinic bifurcation curves $\gamma_{1,\mathrm{crh}}^{\mathrm{hete}}$ and $\gamma_{1,\mathrm{cr}}^{\mathrm{hete}}$ are shown in dashed curves with respect to $\Psi = \pi/6$ and $\Psi = \pi/20$, respectively.

critical homoclinic and heteroclinic bifurcations are the same, and when $0.2408 < \omega \leqslant 1$, the critical heteroclinic bifurcation values are larger than the critical homoclinic bifurcation values.

If the phase shift Ψ is fixed at $\pi/6$ and $\pi/20$, respectively, and the primary optimal control method is employed, then the corresponding control gain G is 2 and 6.3925, respectively. It means the critical homoclinic bifurcation values will be increased, which means that the control regions where the homoclinic transversal intersections do not occur have been enlarged. As can be seen in Fig. 2, in which there are three homoclinic bifurcation curves shown by solid curves, while there are also three heteroclinic bifurcation curve given by dashed curves.

In the following numerical simulation, when the frequency ω is fixed as 0.8, and the corresponding forced amplitude coefficients occurred in the critical homoclinic and heteroclinic bifurcation curves are $A(0.8, \gamma_{1,\mathrm{crh}}^{\mathrm{hom}} = 0.082)$, $B(0.8, 2\gamma_{1,\mathrm{crh}}^{\mathrm{hom}} = 0.1640)$, $C(0.8, 6.3925\gamma_{1,\mathrm{crh}}^{\mathrm{hom}} = 0.5142)$, $D(0.8, \gamma_{1,\mathrm{crh}}^{\mathrm{hete}} = 0.3137)$, $E(0.8, 2\gamma_{1,\mathrm{crh}}^{\mathrm{hete}} = 0.6274)$, and $F(0.8, 6.3925\gamma_{1,\mathrm{crh}}^{\mathrm{hete}} = 2.0053)$, respectively.

3.3. Suppressing homoclinic bifurcations

According to Theorem 1 given in Section 2, in this subsection, the main aim is to compute stable and unstable manifolds of homoclinic orbits and heteroclinic orbits together with other indicators in order to verify the theoretical predictions, in which the perturbed saddles are determined by numerically integrating the perturbed system (16) using Simpson's formula, while the stable and unstable manifolds are detected by a numerical algorithm from [14] based on forward and backward iterations of the unstable and stable eigenvectors, respectively. In the

following numerical simulations, the dark curve represents the stable manifold and the gray curve denotes the unstable manifold.

For simplicity, only a case is considered, that is, the phase shift $\Psi = \pi/6$ is taken, then the control gain is given by $G = 1/|\sin\Psi| = 2$. The main numerical results are listed as below:

(i) Corresponding to the only critical parameter values $\gamma_{1,cr}^{hom} = 2 \times 0.082 = 0.1640 > \gamma_{1,crh}^{hom} = 0.082$ but $\gamma_{1,cr}^{hom} = 0.1640 < \gamma_{1,cr}^{hete} = 0.6274$ in the homoclinic case, the primary resonant optimal control method predicts that the left and right homoclinic manifolds should be in the intersection state, but no such kind of intersection occurred in the heteroclinic manifolds. Fig. 3(a) shows that

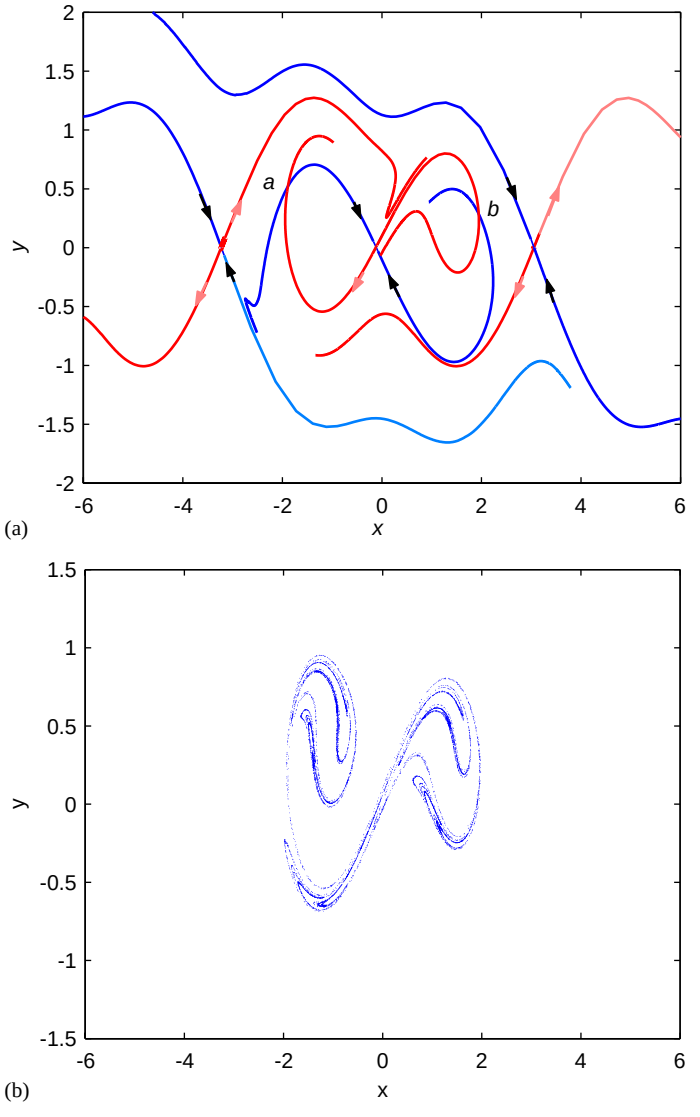

Fig. 3. $\omega = 0.8$, $\alpha = 0.5$, $\delta = 0.1$, $\gamma_1^{hom} = 0.1640$. (a) Numerically computed stable and unstable manifolds; (b) cross-well Duffing-type chaotic attractor.

the numerical results are in good agreement with the theoretical analysis results associated to the three fixed saddle points situated at $S_{-1}(-3.2282, 0.0029)$, $S_0(-0.1176, 0.0054)$, and $S_1(3.0550, 0.0029)$, in which the stable and unstable manifolds of homoclinic orbits at least intersect at points a and b. In addition, corresponding to the same parameters given in Fig. 3(a), Fig. 3(b) shows that there exists only a Duffing-type cross-well chaotic attractor resulting from the homoclinic tangles.

(ii) If the second primary optimal excitation is added to the chaotic system for suppressing the interior homoclinic tangles shown in Fig. 3(a), and the control parameter values are $\gamma_{1,\mathrm{cr}}^{\mathrm{hom}} = 0.1640$ and $\gamma_2^{\mathrm{hom}} = -0.1420$ associated to the three fixed saddle points situated at $S_{-1}(-3.1648, -0.0293)$, $S_0(-0.0323, -0.0394)$, and $S_1(3.1183, -0.0293)$. Then, the left and right homoclinic manifolds should be in the tangency state. Seen from Fig. 4(a), the stable and unstable manifolds of homoclinic orbits are only in the tangency state at points a and b, but a transversal intersection takes place between an unstable manifold of heteroclinic orbit and a stable manifold of homoclinic orbit at point c. The observation demonstrates the suppression for homoclinic transversal intersection occurred in Fig. 3(a) has taken effect, and no such effect for heteroclinic

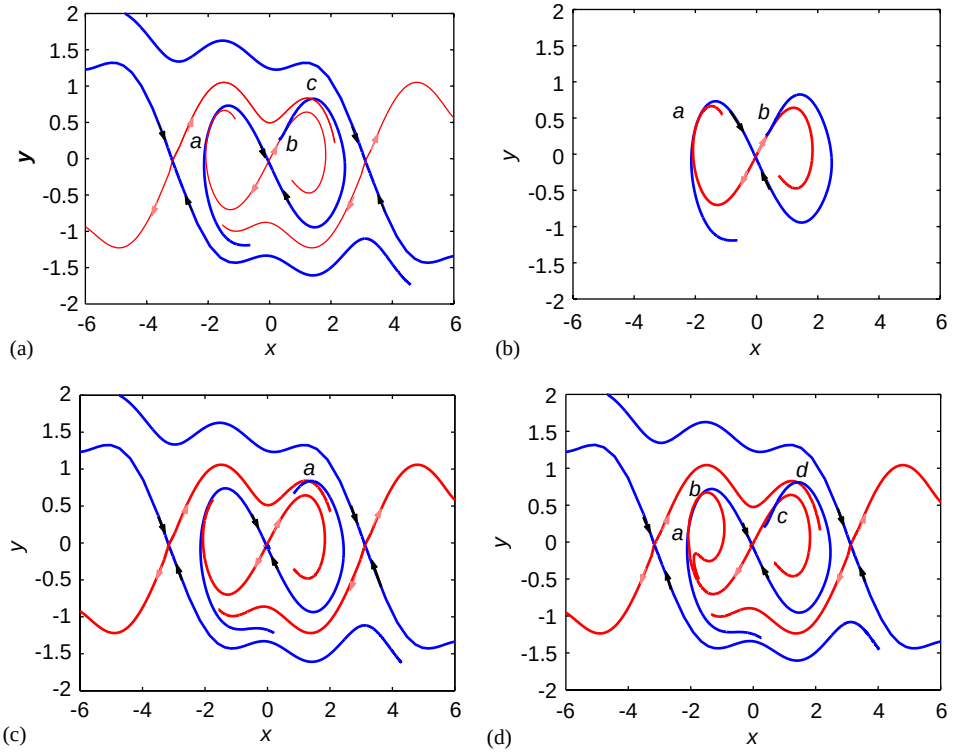

Fig. 4. For $\Psi = \pi/6$, $\omega = 0.8$, $\alpha = 0.5$, $\delta = 0.1$, and $G = 2$. (a) Numerically computed stable and unstable manifolds when $\gamma_1^{\mathrm{hom}} = 0.1640$, $\gamma_2^{\mathrm{hom}} = -0.1420$; (b) the blow-up for homoclinic manifolds given in (a); (c) numerically computed stable and unstable manifolds when $\gamma_1^{\mathrm{hom}} = 0.15$, $\gamma_2^{\mathrm{hom}} = -0.1299$; (d) numerically computed stable and unstable manifolds when $\gamma_1^{\mathrm{hom}} = 0.18$, $\gamma_2^{\mathrm{hom}} = -0.1559$.

manifolds. For the sake of clarity, the blow-up of the homoclinic tangency between the stable and unstable manifolds of homoclinic orbits is given in Fig. 4(b).

(iii) If the first amplitude is just slightly less than the critical value, e.g., $\gamma_1^{\text{hom}} = 0.15$ ($<\gamma_{1,\text{cr}}^{\text{hom}} = 0.1640$) and $\gamma_2^{\text{hom}} = -0.1299$ associated to the three fixed saddle points situated at $S_{-1}(-3.1629, -0.0268)$, $S_0(-0.0296, -0.0360)$, and $S_1(3.1203, -0.0268)$, then the stable and unstable manifolds of homoclinic orbits will be detached as partially shown in Fig. 4(c). But, it is noted that there still exists a transversal intersection between an unstable manifold of heteroclinic orbit and a stable manifold of homoclinic orbit at point a.

(iv) If one takes the first amplitude just slightly larger than the critical value, e.g., $\gamma_1 = 0.18$ ($>\gamma_{1,\text{crh}}^{\text{hom}} = 0.1640$) and $\gamma_2 = -0.1559$ associated to the three fixed saddle points situated at $S_{-1}(-3.1671, -0.0321)$, $S_0(-0.0355, -0.0432)$, and $S_1(3.1161, -0.0321)$, then the stable and unstable manifolds of homoclinic orbits at least intersect at points a, b, and c shown in Fig. 4(d). At the same time, an unstable manifold of heteroclinic orbit and a stable manifold of homoclinic orbit intersect at point d.

Remark. It is noted that the suppression for homoclinic transversal intersections is only a kind of local control instead of the global control since there exist still transversal intersections resulting from the interaction between the interior homoclinic orbits and the outer heteroclinic orbits.

3.4. Suppressing heteroclinic bifurcations

In this subsection, the attention is paid on the suppression for heteroclinic bifurcations using the PROCT presented in this paper. Also, the phase shift is taken as $\Psi = \pi/6$ as that given in Section 3.3. The main results are listed as follows:

(i) When only a critical parameter value $\gamma_1^{\text{hete}} = 2 \times 0.3137 = 0.6274 > \gamma_{1,\text{crh}}^{\text{hete}} = 0.3137$ is taken in the heteroclinic case associated to the three fixed saddle points situated at $S_{-1}(-3.4730, 0.0112)$, $S_0(-0.4499, 0.0207)$, and $S_1(2.8102, 0.0112)$, the PROCT predicts that the left and right heteroclinic manifolds should be in the tangent state, while since the critical heteroclinic bifurcation is greater than the critical homoclinic bifurcation, the interior stable and unstable manifolds of homoclinic orbits should be in the transversal intersection state in theory. Fig. 5(a) shows that the numerical results are in good agreement with the theoretical analysis results, in which the homoclinic tangles, the heteroclinic tangles, and the interwinding homoclinic tangles and heteroclinic tangles take place, which means that there exists a kind of hopping phenomenon of chaos. This result is verified by the plot of strange chaotic attractor given in Fig. 5(b), in which there exist two kinds of basic chaotic attractors, that is Duffing-type and pendulum-type. In addition, two kinds of chaotic attractors interact each other forming a complex compoundable chaotic attractor.

(ii) If the second primary optimal excitation is added to the chaotic system shown in Fig. 5(a), then the control parameter values are $\gamma_1^{\text{hete}} = 0.6274$ and $\gamma_2^{\text{hete}} = -0.5433$ associated to the three fixed saddle points situated at $S_{-1}(-3.2305, -0.1120)$, $S_0(-0.1237, -0.1506)$, and $S_1(3.0527, -0.1120)$, and the left and right heteroclinic manifolds should be in the tangency state in theory. The numerical simulation given in Fig. 5(c) demonstrates that no transversal intersections occur between stable and unstable manifolds of heteroclinic orbit besides a stable

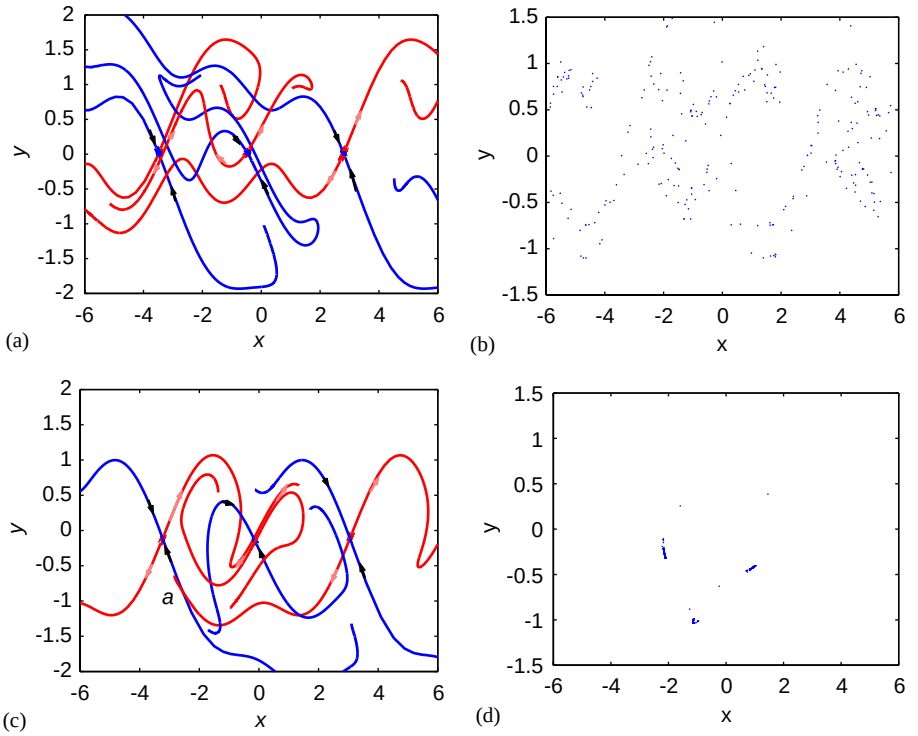

Fig. 5. $\Psi = \pi/6$, $\alpha = 0.5$, $\delta = 0.1$, $\omega = 0.8$, and $G = 2$. (a) Stable and unstable manifolds for $\gamma_1^{\text{hete}} = 0.6274$; (b) interwinding Duffing-type and pendulum-type chaotic attractor for $\gamma_1^{\text{hete}} = 0.6274$; (c) stable and unstable manifolds for $\gamma_1^{\text{hete}} = 0.6274$, $\gamma_2^{\text{hete}} = -0.5433$; (d) three confined chaotic attractors for $\gamma_1^{\text{hete}} = 0.6274$, $\gamma_2^{\text{hete}} = -0.5433$; (e) stable and unstable manifolds for $\gamma_1^{\text{hete}} = 0.6$, $\gamma_2^{\text{hete}} = -0.5196$; (f) quasiperiodic motions for $\gamma_1^{\text{hete}} = 0.6$, $\gamma_2^{\text{hete}} = -0.5196$; (g) stable and unstable manifolds for $\gamma_1^{\text{hete}} = 0.7$, $\gamma_2^{\text{hete}} = -0.6062$; (h) degenerate double Duffing-type cross-well chaotic attractor for $\gamma_1^{\text{hete}} = 0.7$, $\gamma_2^{\text{hete}} = -0.6062$.

manifold of left heteroclinic orbit is only in tangent state with an unstable manifold of right heteroclinic orbits at point a. In addition, since the first amplitude coefficient $\gamma_1^{\text{hete}} = 0.6274$ is largely greater than the critical homoclinic bifurcation $\gamma_1^{\text{hom}} = 0.1640$, seen from Fig. 5(c), there exits very strong transversal intersections between the homoclinic orbits and the homoclinic orbits, as well as the homoclinic orbits and the heteroclinic orbits. That is to say, the suppression is only valid for the heteroclinic bifurcation but it is invalid for the homoclinic bifurcation and the intersection between the homoclinic bifurcation and the heteroclinic bifurcation. But, it is noted that, due to the action played by the PROCT, seen from Fig. 5(d), there exist three confined chaotic attractor occurred in the left, middle, and right sides of phase space plane, respectively. It demonstrates that the hopping phenomenon occurred in Fig. 5(b) has been suppressed in a way.

(iii) If the first amplitude is just slightly less than the critical value, e.g., $\gamma_1^{\text{hete}} = 0.6$ ($< \gamma_1^{\text{hete}} = 0.6274$) and $\gamma_2^{\text{hete}} = -0.5196$ associated to the three fixed saddle points situated at $S_{-1}(-3.2266, -0.1071)$, $S_0(-0.1183, -0.1441)$, and $S_1(3.0566, -0.1071)$, then the stable and unstable manifolds of heteroclinic orbits will be detached as partially in theory. This prediction

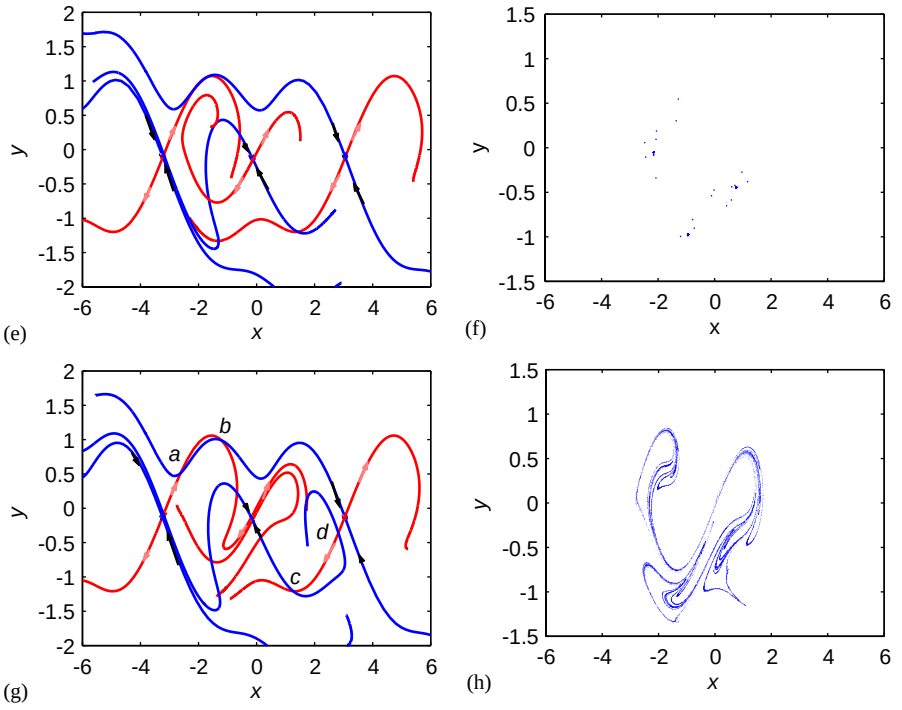

Fig. 5. (*Continued*)

has been confirmed by the numerical results shown in Fig. 5(e), in which the stable and unstable manifolds have been detached, while the stable and unstable manifolds of interior homoclinic orbits are still in the transversal intersection state. There have been no such kind of interaction between the outer heteroclinic orbit and the interior homoclinic orbit. In addition, seen from Fig. 5(f), there exist three quasiperiodic motions in the left, middle, and right sides of phase space.

(iv) If one takes the first amplitude just slightly larger than the critical value, e.g., $\gamma_1 = 0.7$ ($>\gamma_{1,\mathrm{crh}}^{\mathrm{hete}} = 0.8274$) and $\gamma_2 = -0.6062$ associated to the three fixed saddle points situated at $S_{-1}(-3.2408, -0.1249)$, $S_0(-0.1380, -0.1681)$, and $S_1(3.0424, -0.1249)$, then the numerical result is shown in Fig. 5(g), in which, on the one hand, the intensity of homoclinic intersections is a little weaker than those dynamics shown in Fig. 5(a), and on the other hand, an unstable manifold of the left heteroclinic orbit and a stable manifold of the right heteroclinic orbit at least intersect at points a and b. In addition, a stable manifold of the right homoclinic orbit and an unstable manifold of the right heteroclinic orbit at least intersect at points c and d. Fig. 5(h) shows a complicated hopping behavior of cross-well chaotic attractor occurred in the whole phase space, which is a mixture resulting from two interwind Duffing-type chaotic attractors.

4. Conclusions

In this paper, a unified control theorem is presented. The main aim is to suppress the transversal intersections of stable and unstable manifolds of homoclinic and heteroclinic orbits in the

Poincarè map embedding in system dynamics. According to the control theorem, a primary resonant optimal control technique is applied to a general single-dof nonlinear oscillator.

The novelty of this paper is to obtain a unified analytical expression for suppressing the homoclinic and heteroclinic bifurcations. The unified theorem demonstrate that by making use of the phase shift Ψ including the second primary resonant excitation as a original driven control parameter, the control gain G can attain $1/|\sin(\Psi)|$, and $\lim_{\Psi\to 0} G = \infty$ in theory, which will lead to the control region where the homoclinic and heteroclinic bifurcations do not occur can be enlarged as much as possible. Corresponding to those parameters in the control region, the transversal intersections of stable and unstable manifolds of homoclinic and heteroclinic orbits can be successfully avoided.

The technique is applied to a nonlinear oscillator with a pair of nested homoclinic and heteroclinic orbits. By the detailed qualitative analysis and the numerical simulations, the homoclinic and heteroclinic transversal intersections can be suppressed, respectively. In particular, the control scenario discussed in this paper demonstrates that if there exists a pair of homoclinic and heteroclinic orbits, the first choice is to control the homoclinic bifurcation since in general the critical homoclinic bifurcation values are less than the critical heteroclinic bifurcation values. In practice, if the homoclinic transversal intersections can be suppressed, then all transversal intersection occurred in the whole phase space can be controlled, which means that it is a global control strategy.

For the illustrative example discussed in this paper, it is noted that there exists only a kind of chaotic attractor named the Duffing-type only when the homoclinic bifurcations occur. But, if the critical homoclinic bifurcation values are further increased to the critical heteroclinic bifurcation values, then there exist two kinds of interwinding chaotic attractors, that is Duffing-type and pendulum-type, simultaneously. This is a kind of hopping phenomenon. Compared with other hopping behaviors of chaos [13], the hopping behavior shown in this paper is a kind of phenomenon of homoclinic and heteroclinic manifolds intersections. In fact, according to the work of Shaw and Wiggins [15], the kind of hopping phenomenon is rather rare, and the non-interacting chaotic homoclinic and heteroclinic attractors are commonplace.

By using the PROCT proposed in this paper, the hopping behavior of chaos occurred in this paper can be suppressed, and in general it can be transformed into the quasiperiodic motions. On the contrary, if the first amplitude coefficient is greater than the critical heteroclinic bifurcation value, the hopping behavior of chaos will take place again. Therefore, for the example discussed in this paper, the phenomenon of hopping is the dominant type of chaos, whose suppressing or inducing is admissible from the point of practical and theoretical view.

Acknowledgements

This work was supported by the funds of Beijing Jiaotong University (No. RC200300722) and the Natural Science Foundation of Beijing (4052022).

References

[1] Y. Braiman, I. Goldhirsch, Taming chaotic dynamics with weak periodic perturbations, *Physical Review Letters* 66 (1991) 2545–2548.

[2] G. Chen, X. Dong, *From Chaos to Order: Methodologies, Perspectives, and Applications*, World Scientific, Singapore, 1998.
[3] H. Cao, X. Chi, G. Chen, Suppressing or inducing chaos in a model of robot arms and mechanical manipulators, *Journal of Sound and Vibration* 272 (2004) 705–724.
[4] H. Cao, X. Chi, G. Chen, Suppressing or inducing chaos by weak resonant excitations in an externally-forced Froude pendulum, *International Journal of Bifurcation and Chaos* 14 (3) (2004) 1115–1120.
[5] R. Chacón, F. Palmero, F. Balibrea, Taming chaos in a driven Josephson junction, *International Journal of Bifurcation and Chaos* 7 (2001) 1897–1909.
[6] A. Lima, M. Pettini, Suppression of chaos by resonant parametric perturbations, *Physical Review A* 41 (1990) 726–733.
[7] S. Rajasekar, Controlling of chaos by weak periodic perturbations in Duffing–van der Pol oscillator, *Pramana* 41 (1993) 295–309.
[8] J. Guckenheimer, P. Holmes, *Nonlinear Oscillations, Dynamical Systems, and Bifurcations of Vector Fields*, Springer, New York, 1983.
[9] S. Wiggins, *Introduction to Applied Nonlinear Dynamical Systems and Chaos*, Springer, New York, 1990.
[10] S. Lenci, G. Rega, Optimal control of nonregular dynamics in a Duffing oscillator, *Nonlinear Dynamics* 33 (2003) 71–86.
[11] S. Lenci, G. Rega, Optimal control of homoclinic bifurcation: theoretical treatment and practical reduction of safe basin erosion in the Helmholtz oscillator, *Journal of Vibration and Control* 9 (3) (2003) 281–316.
[12] S. Lenci, G. Rega, Heteroclinic bifurcations and optimal control in the nonlinear rocking dynamics of generic and slender rigid blocks, *International Journal of Bifurcation and Chaos*, in press.
[13] M. Dabbs, P. Smith, Critical forcing for homoclinic and heteroclinic orbits of a rotating pendulum, *Journal of Sound and Vibration* 189 (2) (1996) 231–248.
[14] T. Parker, L. Chua, *Practical Numerical Algorithms for Chaotic Systems*, Springer, New York, 1989.
[15] S. Shaw, S. Wiggins, Chaotic dynamics of a whirling pendulum, *Physical D* 31 (1988) 190–211.